

Domain Generalization via Progressive Layer-wise and Channel-wise Dropout

Jintao Guo¹ Lei Qi^{3*} Yinghuan Shi^{1,2*} Yang Gao^{1,2}

¹ National Key Laboratory for Novel Software Technology, Nanjing University

² National Institute of Healthcare Data Science, Nanjing University

³ Key Lab of Computer Network and Information Integration, Southeast University

MF20330025@smail.nju.edu.cn, qilei@seu.edu.cn, syh@nju.edu.cn, gaoy@nju.edu.cn

Abstract

By training a model on multiple observed source domains, domain generalization aims to generalize well to arbitrary unseen target domains without further training. Existing works mainly focus on learning domain-invariant features to improve the generalization ability. However, since target domain is not available during training, previous methods inevitably suffer from overfitting in source domains. To tackle this issue, we develop an effective dropout-based framework to enlarge the region of the model’s attention, which can effectively mitigate the overfitting problem. Particularly, different from the typical dropout scheme, which normally conducts the dropout on the fixed layer, first, we randomly select one layer, and then we randomly select its channels to conduct dropout. Besides, we leverage the progressive scheme to add the ratio of the dropout during training, which can gradually boost the difficulty of training model to enhance the robustness of the model. Moreover, to further alleviate the impact of the overfitting issue, we leverage the augmentation schemes on image-level and feature-level to yield a strong baseline model. We conduct extensive experiments on multiple benchmark datasets, which show our method can outperform the state-of-the-art methods.

1. Introduction

Over the last few years, deep learning has achieved tremendous progress in various vision tasks. However, most existing methods are based on the assumption that training and test samples come from the same data distribution, leading to inferior performance on out-of-distribution data. This phenomenon, known as the problem of domain-shift [28], hinders the applications of deep neural networks because training and test samples are often from different data distributions in real-world scenarios. To overcome this problem, domain adaptation (DA) [10, 23, 45] assumes that the unlabeled target domain can be utilized during the training

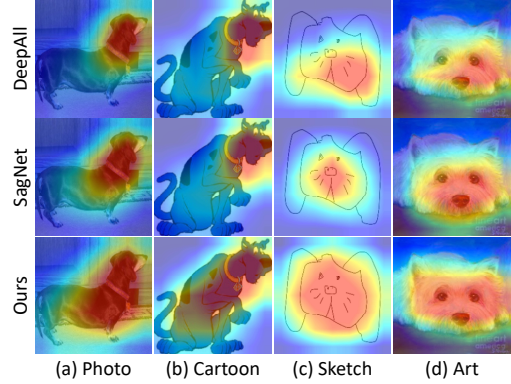


Figure 1. Visualization of different methods using GradCAM [32] on the PACS dataset. Note that the redder the area indicates the higher attention. Top row is the DeepAll, middle row is the SagNet [27] and bottom row is our method. The first three columns are source domains and the last is unseen target domain.

stage to help narrow the potential distribution gap between source and target domains.

However, since collecting data from arbitrary target domains is expensive and impractical, domain generalization (DG) is proposed as a more challenging and practical problem setting, which aims to use multiple source domains to train a model that can generalize well to arbitrary unseen target domains. This setting has aroused wide attention from researchers and many works have been proposed to address DG problem, mainly via domain-invariant learning [16, 29], meta-learning [2, 8], domain augmentation [34, 42], shape-biased learning [27, 43], etc. However, these methods unavoidably face the problem of overfitting in the source domains because the target domain is inaccessible in the training procedure, i.e., the existing methods are inclined to focus on these limited source domains, which will lead to unsatisfactory generalizing ability in unseen target domain.

Our motivation comes from the observation that DeepAll (i.e., a popular baseline in DG) tends to focus on some local regions in source domains, e.g., “head” of dog for photo and cartoon as shown in the top row of Fig. 1. This may lead

*Corresponding author: Yinghuan Shi and Lei Qi.

the model to overfit the sample-specific or domain-specific characteristics. In a nutshell, the model is more likely to focus on the “incorrect” local area on target samples, thus resulting in incorrect predictions. As shown in the middle row of Fig. 1, even for a state-of-the-art DG method, SagNet [27], which could reduce the style bias for learning domain-invariant features, still inevitably suffers from the same overfitting problem. To prevent overfitting to local regions, we expect the model could aware large object regions as much as possible, *e.g.*, “the whole body of dog”, which is achieved by our method as shown in the last row of Fig. 1.

To achieve this goal, in this paper, we propose Progressive LAyer-wise and ChannEl-wise (**PLACE** in short) dropout for domain generalization. The PLACE dropout consists of three components, including the layer-wise selection to drop multi-scale features, the channel-wise dropout to discard different semantic patterns, and the progressive scheme for increasing the ratio of dropout to gradually raise the difficulty of training model. Through our regularization method, the model can adapt to the absence of multi-scale semantic features and avoid overfitting local regions in source domains, so it can focus on large areas when making decisions for target domain. Besides, we propose a strong baseline using augmentation schemes on image-level and feature-level simultaneously, which can promote the data diversity and cooperate with PLACE dropout to help the model learn diverse characteristics. We demonstrate that our PLACE method outperforms several state-of-the-art DG methods on multiple benchmark datasets. Moreover, we conduct experiment to validate that PLACE dropout can narrow the gap between source and target domains via reducing the impact of overfitting source domains.

Our contributions can be summarized as follows:

- We put forward a simple yet effective regularization method for domain generalization, namely *Progressive LAyer-wise and ChannEl-wise dropout* to fight against overfitting, which can randomly drop multi-scale features and different semantic patterns during training. Meanwhile, our method does not introduce any extra network structure in both training and test stage.
- We propose a strong baseline for domain generalization by increasing the data diversity with different augmentation schemes from both image and feature perspectives. Our baseline only involves a few hyper- and no additional training parameters but still achieves a large improvement to the original baseline, *e.g.*, 5.24% (84.92% vs. 79.68%) on PACS with ResNet-18.
- Extensive experiments have demonstrated that our method outperforms several state-of-the-art methods on various benchmark datasets, indicating that alleviating the problem of the overfitting during training can guide the model generalize well to unseen domains.

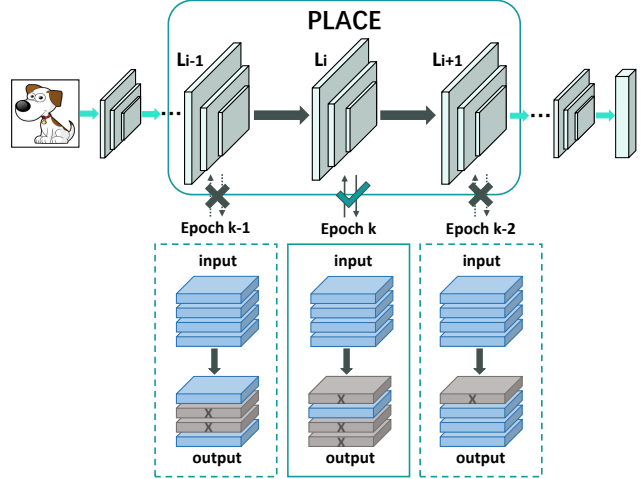


Figure 2. Illustration of the PLACE dropout. Our method contains layer selection and progressive channel-wise dropout. This figure shows the model is trained at the k -epoch and conducts the dropout in the i -th Layer. The detailed procedure is discussed in Sec. 3.2.

2. Related Work

Domain Generalization. Domain generalization (DG) aims to learn a robust model from multiple observed source domains that can generalize to arbitrary unseen domains. Existing DG methods can be roughly divided into three categories of *domain-invariant learning*, *data augmentation* and *regularization methods*. The key idea of domain-invariant learning methods is to learn a shared feature space across observed source domains, which mainly extracts domain-invariant representation via adversarial feature alignment [13, 16], representation disentanglement [6, 29, 44], or meta-learning methods [8, 45]. Domain augmentation is another popular approach that aims to generate out-of-distribution samples, *e.g.*, via domain-adversarial generation [1, 35] or gradient-based adversarial attacks [34, 42]. Recently, some regularization methods have also been proposed to address domain generalization via shape-biased learning [27] or self-supervise methods [4, 43]. Nevertheless, these methods cannot guarantee that features from unseen target domains share the same representation space learned by domain-invariant learning or regularization methods, since the learned model might be overfitting in the source domains due to the absence of target domain. Besides, domain augmentation cannot ensure that the newly generated samples are similar to the target samples [3].

Dropout Regularization. Dropout [36] is one of the most widely used regularization methods to improve the generalization of deep neural networks. In channel-wise and space-wise manners, dropout is developed by Tompson *et al.* [37] to SpatialDropout that drops entire channels in feature maps, and by Ghiasi *et al.* [14] to DropBlock that randomly masks contiguous feature regions, respec-

tively. Recently, many novel dropout methods have been studied, which can be roughly divided into task-auxiliary dropout and structure-information dropout. Task-auxiliary dropout aims to introduce auxiliary tasks to help the model focus on main-task-relevant information [20, 26, 31], *e.g.*, filter dropout [26] which utilizes an auxiliary network to drop the filters responsible for encoding a given sensitive attribute. Structure-information dropout has also been studied to utilize feature-level structure information to guide the dropout during training for a variety of tasks [19, 30, 48]. Unfortunately, previous dropout-based methods could not be directly employed in DG task, as they either need extra network parameters [26, 31] or utilize the guidance that is unsuitable for DG [19, 48]. To mitigate overfitting problem in domain generalization, we design a novel dropout-based framework, which achieves state-of-the-art performance compared with existing DG methods.

3. Proposed Method

3.1. Setting and Overview

Given a training set of multiple observed source domains $\mathcal{D}_S = \{D_1, D_2, \dots, D_K\}$, where K is the number of total source domains, the goal of domain generalization is to learn a domain-agnostic model $f_\theta : \mathcal{X} \rightarrow \mathcal{Y}$ on \mathcal{D}_S , which is expected to generalize well to any unseen target domain D_T without additional training. Moreover, we denote the data space consisting of source domains \mathcal{D}_S as S , and the feature space learned by the model f_θ from \mathcal{D}_S as Z .

Motivated by the observation that local regions are overemphasized which might lead overfitting to source domains, we propose *Progressive LAyer-wise and ChannEl-wise* (**PLACE** in short) dropout to progressively drop channels in the randomly selected layer. The overall framework of PLACE dropout is illustrated in Fig. 2, which can be divided into layer-wise selection and progressive channel-wise dropout. Layer-wise selection is to select the single layer randomly at each iteration. Progressive channel-wise dropout is performed on the feature maps of the selected layer to generate the masked feature vector. This new feature vector is passed to the subsequent layers to compute the loss and update the network. At test time, PLACE dropout is closed as the common dropout. Besides, we design a *strong baseline* for domain generalization to further alleviate the impact of the overfitting issue by increasing the sample diversity with the image-wise and feature-wise augmentations. In the following paragraphs, we introduce the technical details of progressive layer-wise and channel-wise dropout as well as the strong baseline for DG.

3.2. Progressive Layer- and Channel-wise Dropout

Considering that the model tends to overfit source domains, which appears to rely on local regions for prediction

as observed in Fig. 1, we assume that forcing the model to focus on larger regions can effectively mitigate the overfitting problem. To this end, a natural choice is to mask a part of task-relevant features during training and force the model to learn other different discriminative information. Particularly, how to accurately measure the feature importance in DG tasks is still an open problem. Meanwhile, due to the agnosticism of the target domain, existing specifically guided dropout strategies cannot solve the generalization problem well, *e.g.*, over-increasing the difficulty of learning tasks because of discarding too much critical information [18], or effecting little because the guidance is not suitable for DG [48]. To generalize the model to arbitrary target domains, we choose *random* dropout to mask features, thus it can avoid the problem of the guided dropout.

Channel-wise Dropout. Existing dropout methods discard information mainly from channel and spatial levels [26, 30, 48]. In experiments, we find that it is difficult for spatial-wise dropout to choose the locations of dropped areas. If the selected area is in the background, the effect of spatial-wise dropout will decrease. Meanwhile, if the selected area is on the object, it is likely to cause losing too much information and prevent the model from learning discriminative features. Since each channel represents a semantic pattern [37], channel-wise dropout can act on the object more accurately. Moreover, the relationship among channels is weaker than adjacent pixels, which avoids discarding a large contiguous discriminant area and losing too much information. Therefore, we adopt channel-wise dropout to reduce the impact of overfitting.

Given an input of the l -th layer as $\mathbf{F}^l \in \mathbb{R}^{C \times H \times W}$, where H and W denote the dimension of height and width, and C is the number of channels, we firstly generate an all-one mask matrix $\mathbf{M}^l \in \mathbb{R}^{C \times H \times W}$ with the same size as \mathbf{F}^l . Then we randomly sample γ distinct channel indexes $\{r_1, r_2, \dots, r_\gamma\}$ from the C channels of \mathbf{M}^l , where γ is the number of dropped channels. The element in \mathbf{M}^l is set to 0 if it belongs to the selected channels, and set to 1 otherwise:

$$\mathbf{M}_{i,j,k}^l = \begin{cases} 0, & i \in \{r_1, r_2, \dots, r_\gamma\} \\ 1, & \text{otherwise} \end{cases}. \quad (1)$$

The masked input for the l -th layer is obtained by element-wise multiplication of the input and mask matrix:

$$\widehat{\mathbf{F}}^l = \mathbf{F}^l \odot \mathbf{M}^l, \quad (2)$$

Layer-wise Dropout. Different from most previous dropout methods by conducting the dropout on a fixed layer, we propose *layer-wise dropout* which randomly selects a middle layer of the network and performs progressive channel-wise dropout on its feature maps at each iteration. Since feature representation in different layers shows a large diversity, setting dropout in different layers has var-

ious effects on the performance as demonstrated in our experiments. However, the simultaneous usage of dropout in multiple layers may result in the absence of too much information during training, which could prevent the model from learning discriminatory information from source domains. To avoid this problem, our *layer-wise dropout* conducts dropout in a different single layer at each iteration, thus protecting the model from losing too much information at once. Moreover, performing the dropout in different layers means dropping multi-scale features during training, which can force the model to focus on larger regions, and thus it is beneficial to alleviate the overfitting problem.

Progressive Scheme. We design *progressive scheme* that drops channels progressively to ensure the stability of model convergence and force the model to focus on large regions, which eases the overfitting issue more adequately. It is motivated by the observation that fixed-proportion dropout makes the model difficult to converge in its early training stage, which is harmful to its final performance. Given the current epoch number e , we compute the dropout radio P and the number of dropped channels γ as below:

$$\gamma = C \times P = C \times P_{max} \times G(e), \quad (3)$$

where P_{max} denotes the maximum of channel-wise dropout radio, and C is the number of channels. $G(\cdot)$ could be an appropriate monotonically increasing function with e as input and a value from 0 and 1 as output. We empirically adopt the arctangent function (*i.e.*, $\arctan(\cdot)$) as Eq. (4) for $G(\cdot)$ in our experiments, where V is a hyper-parameter to control the increasing speed of P :

$$G(e) = \frac{2}{\pi} \arctan\left(\frac{e}{V}\right). \quad (4)$$

The overall training procedure of PLACE dropout is summarized in Algorithm 1. In the training stage, our method encourages the network to classify samples based on large regions for mitigating overfitting in source domains. During the inference process, our PLACE dropout is closed as conventional dropout. It is worth noting that the PLACE dropout only comprises a few simple operations, such as random selection and channel-wise product so that no additional parameters are introduced during training.

Discussion. Our method differs from RSC [18], which discards the features with high gradients to force the model to predict with remaining information, in three aspects. 1) Different from that fixed proportion of neurons are dropped in RSC, our approach adopts a progressive strategy to increase the proportion, which can activate the model more adequately. 2) Compared with RSC in which only the neurons in the last layer before the classifier are masked, PLACE dropout drops channels in the middle layers, which is beneficial to the training of the shallow layers. 3) Spatial- or channel-wise features with high gradients are

Algorithm 1: PLACE dropout Algorithm

Input: Batch size N , learning rate η , source data $\{(x_k, y_k)\}$, candidate layer set $\{l_1, \dots, l_n\}$, updated network f_{θ_u} .
Output: Trained network $f_{\theta_u^*}$.
for sampled mini-batch $\{(x_k, y_k)\}_{k=1}^N$ **do**
 Sample l from $\{l_1, \dots, l_n\}$;
 $\mathbf{F}^l \leftarrow$ Computed by forward propagation ;
 P and $\gamma \leftarrow$ Computed by Eq. (3) ;
 for each sample (x_i, y_i) **do**
 Randomly sample γ channels from F_i^l ;
 $\mathbf{M}_i^l \leftarrow$ Computed by Eq. (1) ;
 $\widehat{\mathbf{F}}^l \leftarrow$ Computed by Eq. (2) ;
 end
 Update $\mathbf{F}^l \leftarrow \widehat{\mathbf{F}}^l$;
 Compute the output of the succeeding layers ;
 Compute $L \leftarrow -\frac{1}{N} \sum_{i=1}^N \sum_{k=1}^K y_{ik} \log(p_{ik})$;
 Update $\theta_u \leftarrow \theta_u - \eta \nabla_{\theta_u} L$;
end

dropped randomly in RSC. However, we find that in PLACE dropout, only dropping channel-wise features is more effective for alleviating the overfitting issue in source domains.

3.3. Strong Baseline for Domain Generalization

Our PLACE method imposes an implicit constraint that requires the model to extend the feature space Z extracted from the source data space S . To further achieve this objective, we here attempt to diversify the source space S to enlarge the feature space Z . Specifically, we put forward a *strong baseline model* for domain generalization with image-level and feature-level augmentation methods. By enlarging the space, our strong baseline could aid in learning more informative features. In this sense, based on our strong baseline, PLACE dropout is expected to show a better ability to resist overfitting than the conventional way.

Image-level Augmentation. RandAugment [7] is an effective automatic data augmentation method to increase diversity. From 14 available transformations, α transformations are selected and the magnitude of each augmentation distortion is set as β . The parameters α and β are human-interpretable [7] such that larger values of α and β increase regularization strength. We observed that RandAugment could promote data diversity while enhancing the generalization ability of the model meanwhile. Hence, we propose to use RandAugment to increase the image-level diversity.

Feature-level Augmentation. Instance-specific mean and standard deviation are usually used to represent image style, which has been validated in style transfer models [11, 17, 39, 40]. Given an input image x , the feature

maps of x can be denoted as $F_x \in \mathbb{R}^{C \times H \times W}$, with H and W as the dimension of height and width, C as the number of channels, respectively. We denote the channel-wise mean and standard deviation of F_x as F_μ and F_σ , calculated as:

$$F_\mu = \frac{1}{HW} \sum_{h=1}^H \sum_{w=1}^W F_{c,h,w}, \quad (5)$$

$$F_\sigma = \sqrt{\frac{1}{HW} \sum_{h=1}^H \sum_{w=1}^W ((F_{c,h,w} - F_\mu)^2)}. \quad (6)$$

Besides, in AdaIN [17], the mean and standard deviation of original image are replaced by that of style image y (denoted as (S_μ, S_σ)) to achieve arbitrary style transfer as:

$$\text{AdaIN}(x, y) = S_\sigma \frac{F_x - F_\mu}{F_\sigma} + S_\mu. \quad (7)$$

Inspired by AdaIN, we utilize a style diversification module, namely *SwapStyle*, which swaps style statistics for any two pictures randomly during training to augment source feature space from the feature level. The formula is defined as:

$$\begin{aligned} (\hat{x}, \hat{y}) &= \text{SwapStyle}(x, y), \\ &= (\text{AdaIN}(x, y), \text{AdaIN}(y, x)). \end{aligned} \quad (8)$$

Discussion. Particularly, SwapStyle is essentially different from MixStyle [51]. MixStyle aims to enhance the robustness of model to domain-shift by mixing the feature statistics of two samples from different domains. However, overfitting problem does not only exist at the domain level, but also at the image level. Considering that RandAugment brings large images-wise differences, we swap the feature statistics between any two source images to further increase the difference among samples. Moreover, we find from experiments that swapping styles can mitigate the overfitting more effectively than mixing styles because it modifies the image style information more obviously. Consequently, SwapStyle can cooperate with RandAugment to enrich the data space and mitigate the overfitting more adequately.

4. Experiments and Results

4.1. Datasets and Settings

We evaluate our method on three popularly-used DG benchmark datasets including:

PACS [21] consists of images from 4 domains: **Photo**, **Art Painting**, **Cartoon** and **Sketch**, including 7 object categories and 9,991 images totally. We use the official train-validation split provided by [21] for training and validation.

VLCS [38] comprises of 5 categories selected from four domains, **VOC 2007** (Pascal), **LabelMe**, **Caltech** and **Sun**. We utilize the same experimental setup as [4] and divide the dataset into training and validation sets based on 7 : 3.

Office-Home [41] contains around 15,500 images of 65 categories from four domains namely **Artistic**, **Clipart**, **Product** and **Real-World**. Follow [4], we randomly split each domain into 90% for training and 10% for validation.

We apply the leave-one-domain-out protocol for all benchmarks, *i.e.*, we train the model in source domains and test the model in the remaining domain. Due to the progressive scheme, we select the model of the last epoch as the final model and report the top-1 classification accuracy. All the reported results are the averaged value over five runs.

4.2. Implementation Details

For PACS, we use the ImageNet pretrained ResNet-18 and ResNet-50 as backbones following [15] and adopt the same hyper-parameters as [4]. For VLCS, We employ the experimental protocol as mentioned in [49] and use ResNet-18 as backbone. For OfficeHome, we follow the same experimental setup as [12]. We train the network using SGD with a momentum of 0.9 and weight decay of $5e - 4$ for a total of 60 epochs, where the first 30 epochs are considered as stage 1 to get the trained baseline model and the next 30 epochs are stage 2 to further mitigate the overfitting issue.

For each iteration, we select 64 samples and concatenate their standard augmentations [4] and random augmentations [7] together to generate a batch of 128. The initial learning rate of the whole network is $1e - 3$ and decayed by 0.1 at 80% of the total epochs for both stages. For all experiments, we set the number of transformations γ as 8 and distortion magnitude β as 4 in RandAugment. The maximum of dropout radio P_{max} is set as 0.33 both for PACS and VLCS, and 0.25 for OfficeHome, respectively. The progressive rate V of dropout is set as 4 in all datasets.

4.3. Comparison with SOTA Methods

PACS. The results are presented in Tab. 1. Our method achieves the best performance on both backbones. Compared with MetaAlign [45], the latest meta-learning method that treats the domain alignment and the classification objective as the meta-train and meta-test tasks, our method improves 4.43% (86.33% vs. 81.90%) on ResNet-18. Our method also exceeds the second-best method FACT [47], the state-of-the-art shape-biased model utilizing Fourier-based augmentation to force the model to capture semantics, by 0.49% (88.64% vs. 88.15%) on ResNet-50, illustrating that our method can learn more discriminative features.

VLCS. The results are shown in Tab. 2. Our method exceeds the SOTA method StableNet [49] by 0.11% (77.76% vs. 77.65%) on average. Specifically, our method precedes StableNet on Caltech and Pascal with a considerable improvement of 1.56% (98.23% vs. 96.67%) and 2.71% (76.30% vs. 73.59%) respectively, but slightly inferior to it on the other two domains. This can be interpreted as our method drops task-relevant features randomly to mitigate

Table 1. Comparison of performance (%) among different methods using ResNet-18 and ResNet-50 on PACS [21] (Best in **bold**).

Method	Art	Cartoon	Sketch	Photo	Avg.
ResNet-18					
Deep All	78.63	75.27	68.72	96.08	79.68
DMG [5]	76.90	80.38	75.21	93.35	81.46
MMLD [25]	81.28	77.16	72.29	96.09	81.83
L2A-OT [50]	83.30	78.20	73.60	96.20	82.80
DSON [33]	84.67	77.65	82.23	95.87	85.11
MixStyle [51]	84.10	78.80	75.90	96.10	83.70
COPA [46]	83.30	79.80	82.50	94.60	85.10
LDSDG [44]	81.44	79.56	80.58	95.51	84.27
NAS-OoD [1]	83.74	79.69	77.27	96.23	84.23
SFA-A [22]	81.20	77.80	73.70	93.90	81.70
SagNet [27]	83.58	77.66	76.30	95.47	83.25
FACT [47]	85.37	78.38	79.15	95.15	84.51
DAML [35]	83.00	78.10	74.10	95.60	82.70
StableNet [49]	81.74	79.91	80.50	96.53	84.69
RSC [18]	83.43	80.31	80.85	95.99	85.15
RSC (<i>our imple.</i>)	82.03	77.39	75.64	95.63	82.67
MetaNorm [9]	85.01	78.63	83.17	95.99	85.70
MDGHybrid [24]	82.80	81.61	81.05	96.67	85.53
Ours	84.83	80.12	83.68	96.69	86.33
ResNet-50					
Deep All	81.31	78.54	69.76	94.97	81.15
MASF [8]	82.89	80.49	72.29	95.01	82.67
MetaReg [2]	87.20	79.20	70.30	97.60	83.60
DMG [5]	82.57	78.11	78.32	94.49	83.37
EISNet [43]	86.64	81.53	78.07	97.11	85.84
DSON [33]	87.04	80.62	82.90	95.99	86.64
RSC [18]	87.89	82.16	83.85	97.92	87.83
RSC (<i>our imple.</i>)	84.13	79.83	82.32	95.35	85.41
MDGHybrid [24]	86.74	82.32	82.66	98.36	87.52
FACT [47]	89.63	81.77	84.46	96.75	88.15
Ours	89.44	81.61	85.88	97.62	88.64

Table 2. Comparison of performance (%) among different methods using ResNet-18 on VLCS [38] (Best in **bold**).

Method	Caltech	LabelMe	Pascal	Sun	Avg.
Deep all	91.86	61.81	67.48	68.77	72.48
JiGen [4]	96.17	62.06	70.93	71.40	75.14
MMLD [25]	97.01	62.20	73.01	72.49	76.18
RSC [18]	96.21	62.51	73.81	72.10	76.16
RSC (<i>our imple.</i>)	95.83	63.74	71.86	72.12	75.89
StableNet [49]	96.67	65.36	73.59	74.97	77.65
Ours	98.23	64.38	76.30	72.12	77.76

overfitting while StableNet [49] discards the task-irrelevant features for stable learning, causing their different effects on generalization performance of the model.

OfficeHome. The results are reported in Tab. 3. Our method exceeds the latest DG methods, *e.g.*, COPA [46] by 0.72% (66.82% vs. 66.10%) and FACT [47] by 0.26% (66.82% vs. 66.56%). Although Clipart is dissimilar to

Table 3. Comparison of performance (%) among different methods using ResNet-18 on Office-Home [41] (Best in **bold**).

Method	Artistic	Clipart	Product	Real	Avg.
Deep All	52.06	46.12	70.45	72.45	60.27
D-SAM	58.03	44.37	69.22	71.45	60.77
Jigen [4]	53.04	47.51	71.47	72.79	61.20
DSON [33]	59.37	45.70	71.84	74.68	62.90
L2A-OT [50]	60.60	50.10	74.80	77.00	65.60
MetaNorm [9]	59.77	45.98	73.13	75.29	63.55
SagNet [27]	60.20	45.38	70.42	73.38	62.34
RSC [18]	58.42	47.90	71.63	74.54	63.12
RSC (<i>our imple.</i>)	57.70	48.58	72.59	74.17	63.26
COPA [46]	59.40	55.10	74.80	75.00	66.10
FACT [47]	60.34	54.85	74.48	76.55	66.56
Ours	59.79	57.07	74.14	76.29	66.82

other domains and also more difficult to generalize, our method still achieves a improvement of 1.97% (57.07% vs. 55.10%) over the nearest competitor COPA [46].

Compared with RSC [18][†], which is most relevant to our method and utilizes the gradient-guided dropout to improve generalization, our method gains a large improvement on all datasets, *e.g.*, 3.66% (86.33% vs. 82.67%) with ResNet-18 and 3.23% (88.64% vs. 85.41%) with ResNet-50 on PACS, 1.87% (77.76% vs. 75.89%) on VLCS and 3.56% (66.82% vs. 63.26%) on OfficeHome. The stable improvements reveal that PLACE dropout can boost the robustness of the model better than RSC via mitigating the overfitting issue of the model in source domains.

Overall, all of the above comparisons reveal the effectiveness and superiority of our approach to other state-of-the-art domain generalization methods and demonstrate that our method is capable of alleviating overfitting problem in source domains and promoting the generalization capacity on arbitrary unseen target domains.

4.4. Ablation Studies

Effect of different components in PLACE dropout.

We conduct ablation studies to demonstrate the importance of each component in PLACE dropout. As shown in Tab. 4, the absence of layer-wise dropout causes an obvious decline of 1.19% (84.66% vs. 83.47%) on DeepAll and 0.58% (86.33% vs. 85.75%) on DeepAll⁺⁺. Besides, progressive scheme brings an improvement of 0.51% (84.66% vs. 84.15%) on DeepAll and 0.48% (86.33% vs. 85.85%) on DeepAll⁺⁺. The channel-wise dropout also plays an important role in PLACE dropout, which gains 0.6% (84.66% vs. 84.06%) on DeepAll and 0.92% (86.33% vs. 85.41%) on DeepAll⁺⁺. As a whole, the PLACE dropout lifts the performance by 4.98% (84.66% vs. 79.68%) versus DeepAll

[†]We rerun the official codes of RSC with the same hyperparameters as mentioned in [18] but fail to reproduce the reported results, which may be due to the different hardware environment. This problem is also reported in [47]. To be fair, we compare our method with RSC in our environment.

Table 4. Effect (%) of each components in PLACE dropout on the PACS dataset with ResNet-18. We denote layer-wise dropout as L, progressive scheme as P and channel-wise dropout as C. DeepAll⁺⁺ means DeepAll with SwapStyle and RandAugment.

Method	Art	Cartoon	Sketch	Photo	Avg.
DeepAll	78.63	75.27	68.72	96.08	79.68
+ PLACE w/o. L	83.84	75.89	77.78	96.37	83.47
+ PLACE w/o. P	83.62	78.01	78.17	96.79	84.15
+ PLACE w/o. C	83.59	76.32	78.98	97.37	84.06
+ PLACE	83.74	80.84	77.58	96.47	84.66
DeepAll ⁺⁺	83.64	78.28	81.41	96.34	84.92
+ PLACE w/o. L	84.74	79.77	82.11	96.37	85.75
+ PLACE w/o. P	84.53	79.83	82.56	96.48	85.85
+ PLACE w/o. C	83.77	79.02	82.51	96.35	85.41
+ PLACE	84.83	80.12	83.68	96.69	86.33

and 1.41% (86.33% vs. 84.92%) versus DeepAll⁺⁺. All components can increase obvious improvement on both DeepAll and DeepAll⁺⁺, suggesting the effectiveness of each component to promote the generalization of the model.

Effect of PLACE dropout on different baselines. We perform ablation studies to quantify the impact of RandAugment and SwapStyle on DeepAll and prove the effectiveness of PLACE dropout on different baselines. As presented in Fig. 3, we apply PLACE dropout to DeepAll (D) and gain an improvement of 4.98% (84.66% vs. 79.68%), which already performs better than many latest works, *e.g.*, NAS-OoD [1] and SFA-A [22] in Tab. 1. Our method exceeds RSC [18] by 1.99% (84.66% vs. 82.67%), showing that our method effectively promotes generalization on DeepAll. Subsequently, we combine DeepAll with SwapStyle(S) or RandAugment(R), which enhance the performance by 2.82% (82.50% vs. 79.68%) and 3.95% (83.63% vs. 79.68%) respectively. This validates the effectiveness of SwapStyle and RandAugment when we increase feature- and image-level diversity. PLACE dropout obtains a clear improvement on the two models, *e.g.*, 3.14% (85.64% vs. 82.50%) for SwapStyle and 1.39% (85.02% vs. 83.63%) for RandAugment. Combining DeepAll with SwapStyle and RandAug, we obtain the strong baseline lifting the performance by 5.24% (84.92% vs. 79.68%). Based on this baseline, PLACE dropout improves by 1.41% (86.33% vs. 84.92%). The results verify the stable effectiveness of PLACE dropout on various baselines.

Effect of Two-stages training scheme. It is worth noting that we train the model with two stages, where the first is to warm up the model and the second is to progressively enhance the resistance of the model to overfitting. We test the one-stage scheme, *i.e.*, applying PLACE dropout to the model at the beginning and training as the same epoch as the two-stages scheme. The results show that although PLACE dropout is still useful in one-stage training with an enhancement of 0.84% (85.86% vs. 84.92%), our method can ob-

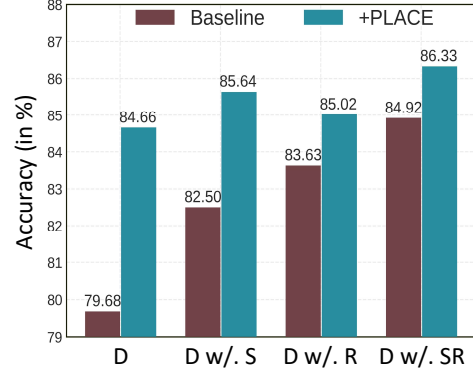


Figure 3. Abaration studies (%) on different components of our method on the PACS dataset with ResNet-18.

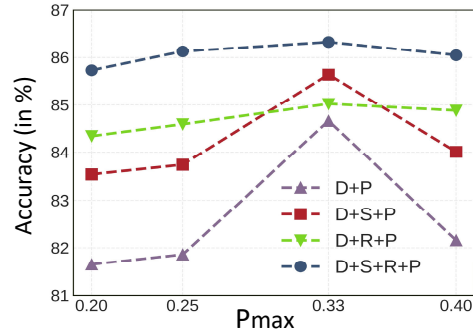


Figure 4. Effect (%) of different P_{\max} in PLACE dropout to performance on different baselines.

tain a larger improvement by 1.41% (86.33% vs. 84.92%) in two-stages training. This is explainable that warming up the model can obtain the good initialization parameters before we train the model using the PLACE dropout, thereby getting the better generalization capability.

5. Discussion

Where to apply PLACE dropout. We train the model with PLACE dropout in different layers of ResNet-18 on PACS. The results are shown in Tab. 5. We observe that applying PLACE dropout to higher-level layers generally achieves better performance, *e.g.*, L3 is better than L2 (86.08% vs. 85.31%). The performance declines when applying PLACE dropout to L4 alone, which is reasonable that L4 is near the prediction layer of the network, and the update parameters may not be enough. Applying PLACE dropout to L3 and L4 achieves the best performance (86.33%) among all schemes. This makes sense because L3 and L4 have larger receptive fields and capture more semantic information. As a consequence, applying PLACE dropout to L3 and L4 randomly can force the model to focus more effectively on large regions.

How to set the maximum dropping proportion. P_{\max}

Table 5. Effect (%) of different layers where the PLACE dropout is inserted on PACS with ResNet-18. For notation, L1 means PLACE dropout is applied after the first residual block; layer set {L1, L2} means PLACE dropout is applied after the first or the second residual blocks randomly.

L1	L2	L3	L4	Art	Cartoon	Sketch	Photo	Avg.
-	-	-	-	96.34	83.64	78.28	81.41	84.92
✓	-	-	-	83.71	78.18	85.03	95.53	85.61
-	✓	-	-	83.59	78.91	83.45	95.31	85.31
-	-	✓	-	84.73	80.08	82.87	96.65	86.08
-	-	-	✓	83.76	78.23	82.14	96.39	85.13
✓	✓	-	-	82.92	78.26	84.72	95.37	85.32
-	✓	✓	-	84.86	79.66	83.29	96.31	86.03
-	-	✓	✓	84.83	80.12	83.68	96.69	86.33
✓	✓	✓	-	84.33	79.68	84.64	95.99	86.16
-	✓	✓	✓	84.72	79.42	83.06	96.05	85.81
✓	✓	✓	✓	84.81	80.09	83.74	95.91	86.14

is a hyper-parameter in our method, which means the maximum proportion of dropping channels (Eq. (3)). We conduct experiments with four baseline models on PACS, DeepAll (D), DeepAll with SwapStyle (D + S), DeepAll with RandAugment (D + R) and DeepAll with SwapStyle and RandAugment (D + S + R). Our PLACE dropout is denoted as P and the results are shown in Fig. 1. It is clear that all of the models achieve the best performance when P_{\max} is set as 0.33 but perform worse when P_{\max} is neither too large nor too small. Too large P_{\max} may cause missing too much information during training, which hinders the model to learn discriminatory information from source domains. Too small P_{\max} may make the model fail to adequately alleviate the overfitting. P_{\max} is also determined in this way for other datasets, 0.33 for VLCS and 0.25 for OfficeHome.

Effect of SwapStyle. We conduct experiments to compare SwapStyle with MixStyle [51] on DeepAll and the stronger DeepAll (with RandAugment). The results are represented in Tab. 6. As seen, MixStyle achieves the best performance on DeepAll, *e.g.*, outperforms SwapStyle by 0.30% (82.80% vs. 82.50%). However, on the stronger DeepAll with RandAugment, SwapStyle performs better than MixStyle and improves the performance by a margin of 0.66% (84.92% vs. 84.26%). The results align well with the discussion in Section 3.3 and demonstrate that SwapStyle can cooperate with RandAugment to better enlarge the data space, so that alleviate the overfitting problem in source domains more adequately.

Distribution discrepancy of feature representations. We examine the inter-domain (across all source domains) and intra-class (inter-domain distance for the same-class samples) discrepancy to investigate the influence of PLACE dropout, as reported in Tab. 2. In our experiments, the inter-domain discrepancy is measured by the distance $d_{inter-domain} = \frac{2}{K(K-1)} \sum_{m \neq n}^K \|\bar{X}_m - \bar{X}_n\|_2$, where K denotes the number of source domains, \bar{X}_m and \bar{X}_n

Table 6. Effect (%) of SwapStyle and MixStyle on DeepAll and DeepAll with RandAugment. We denote RandAugment as R.

Method	Art	Cartoon	Sketch	Photo	Avg.
DeepAll	78.63	75.27	68.72	96.08	79.68
+ MixStyle	82.30	79.00	73.80	96.30	82.80
+ SwapStyle	81.47	77.76	74.34	96.43	82.50
DeepAll w. R	82.90	76.89	78.55	96.17	83.63
+ MixStyle	84.08	76.37	80.43	96.17	84.26
+ SwapStyle	83.64	78.28	81.41	96.34	84.92

Table 7. The distribution discrepancy ($\times 10$) of inter-domain (across all source domains) and intra-class (for all classes in source domains) on PACS. Note that the lower the value indicates the better performance.

Method	Inter-domain	Intra-class
DeepAll	2.43	2.95
+ PLACE	1.96	2.48
DeepAll w. S	1.99	2.52
+ PLACE	1.91	2.43
DeepAll w. R	2.05	2.50
+ PLACE	1.86	2.34
DeepAll ⁺⁺	1.63	2.13
+ PLACE	1.53	2.04

denote the sample mean of the m -th and n -th source domains respectively. To measure the intra-class discrepancy, we use $d_{intra-class} = \frac{1}{CK} \sum_{c=1}^C \sum_{k=1}^K \|\bar{X}_{k,c} - \bar{X}_k\|_2$, where $\bar{X}_{k,c}$ is the sample mean of the c -th class in the k -th source domain and C is the number of categories. These distances are calculated in Tab. 2. The inter-domain distance of DeepAll is larger than that of all our baselines, proving that RandAugment and SwapStyle can both reduce the discrepancy among source domains and cooperate to narrow the domain gap. Moreover, the inter-domain distance of PLACE dropout is always smaller than that of all baselines, indicating its ability of reducing domain discrepancy on different baselines. For intra-class discrepancy, DeepAll⁺⁺ achieves smaller distances than DeepAll because DeepAll⁺⁺ can augment source data space to mitigate the overfitting. Among all of the results, our PLACE dropout reaches the smallest distance, proving its best capability of reducing intra-class discrepancy in source domains.

6. Conclusion

In this paper, we propose an effective dropout-based training framework for domain generalization which alleviates overfitting in source domains and helps the model generalize well in unseen target domain. Extensive experiments on multiple benchmarks prove the effectiveness of our method, which achieves state-of-the-art performance compared with existing domain generalization approaches.

References

- [1] Haoyue Bai, Fengwei Zhou, Lanqing Hong, Nanyang Ye, S-H Gary Chan, and Zhenguo Li. Nas-ood: Neural architecture search for out-of-distribution generalization. In *Proceedings of the IEEE/CVF International Conference on Computer Vision*, pages 8320–8329, 2021. [2](#), [6](#), [7](#)
- [2] Yogesh Balaji, Swami Sankaranarayanan, and Rama Chellappa. Metareg: Towards domain generalization using meta-regularization. *Advances in Neural Information Processing Systems*, 31:998–1008, 2018. [1](#), [6](#)
- [3] David Berthelot, Colin Raffel, Aurko Roy, and Ian Goodfellow. Understanding and improving interpolation in autoencoders via an adversarial regularizer. *arXiv preprint arXiv:1807.07543*, 2018. [2](#)
- [4] Fabio M Carlucci, Antonio D’Innocente, Silvia Bucci, Barbara Caputo, and Tatiana Tommasi. Domain generalization by solving jigsaw puzzles. In *Proceedings of the IEEE/CVF Conference on Computer Vision and Pattern Recognition*, pages 2229–2238, 2019. [2](#), [5](#), [6](#), [11](#)
- [5] Prithvijit Chattopadhyay, Yogesh Balaji, and Judy Hoffman. Learning to balance specificity and invariance for in and out of domain generalization. In *European Conference on Computer Vision*, pages 301–318. Springer, 2020. [6](#)
- [6] Yang Chen, Yu Wang, Yingwei Pan, Ting Yao, Xinmei Tian, and Tao Mei. A style and semantic memory mechanism for domain generalization. In *Proceedings of the IEEE/CVF International Conference on Computer Vision*, pages 9164–9173, 2021. [2](#)
- [7] Ekin D Cubuk, Barret Zoph, Jonathon Shlens, and Quoc V Le. Randaugment: Practical automated data augmentation with a reduced search space. In *Proceedings of the IEEE/CVF Conference on Computer Vision and Pattern Recognition Workshops*, pages 702–703, 2020. [4](#), [5](#), [11](#)
- [8] Qi Dou, Daniel Coelho de Castro, Konstantinos Kamnitsas, and Ben Glocker. Domain generalization via model-agnostic learning of semantic features. *Advances in Neural Information Processing Systems*, 32:6450–6461, 2019. [1](#), [2](#), [6](#)
- [9] Yingjun Du, Xiantong Zhen, Ling Shao, and Cees GM Snoek. Metanorm: Learning to normalize few-shot batches across domains. In *International Conference on Learning Representations*, 2020. [6](#)
- [10] Zhekai Du, Jingjing Li, Hongzu Su, Lei Zhu, and Ke Lu. Cross-domain gradient discrepancy minimization for unsupervised domain adaptation. In *Proceedings of the IEEE/CVF Conference on Computer Vision and Pattern Recognition*, pages 3937–3946, 2021. [1](#)
- [11] Vincent Dumoulin, Jonathon Shlens, and Manjunath Kudlur. A learned representation for artistic style. *arXiv preprint arXiv:1610.07629*, 2016. [4](#)
- [12] Antonio D’Innocente and Barbara Caputo. Domain generalization with domain-specific aggregation modules. In *German Conference on Pattern Recognition*, pages 187–198. Springer, 2018. [5](#), [11](#)
- [13] Xinjie Fan, Qifei Wang, Junjie Ke, Feng Yang, Boqing Gong, and Mingyuan Zhou. Adversarially adaptive normalization for single domain generalization. In *Proceedings of the IEEE/CVF Conference on Computer Vision and Pattern Recognition Workshops*, pages 32–33, 2020. [3](#)
- [14] Golnaz Ghiasi, Tsung-Yi Lin, and Quoc V Le. Dropblock: A regularization method for convolutional networks. *arXiv preprint arXiv:1810.12890*, 2018. [2](#)
- [15] Kaiming He, Xiangyu Zhang, Shaoqing Ren, and Jian Sun. Deep residual learning for image recognition. In *Proceedings of the IEEE conference on computer vision and pattern recognition*, pages 770–778, 2016. [5](#)
- [16] Dan Hendrycks, Mantas Mazeika, Saurav Kadavath, and Dawn Song. Using self-supervised learning can improve model robustness and uncertainty. *Advances in Neural Information Processing Systems*, 32:15663–15674, 2019. [1](#), [2](#)
- [17] Xun Huang and Serge Belongie. Arbitrary style transfer in real-time with adaptive instance normalization. In *Proceedings of the IEEE International Conference on Computer Vision*, pages 1501–1510, 2017. [4](#), [5](#)
- [18] Zeyi Huang, Haohan Wang, Eric P Xing, and Dong Huang. Self-challenging improves cross-domain generalization. In *Computer Vision–ECCV 2020: 16th European Conference, Glasgow, UK, August 23–28, 2020, Proceedings, Part II 16*, pages 124–140. Springer, 2020. [3](#), [4](#), [6](#), [7](#), [12](#)
- [19] Zhiwei Ke, Zhiwei Wen, Weicheng Xie, Yi Wang, and Linlin Shen. Group-wise dynamic dropout based on latent semantic variations. In *Proceedings of the AAAI Conference on Artificial Intelligence*, volume 34, pages 11229–11236, 2020. [3](#)
- [20] Rohit Keshari, Richa Singh, and Mayank Vatsa. Guided dropout. In *Proceedings of the AAAI Conference on Artificial Intelligence*, volume 33, pages 4065–4072, 2019. [3](#)
- [21] Da Li, Yongxin Yang, Yi-Zhe Song, and Timothy M Hospedales. Deeper, broader and artier domain generalization. In *Proceedings of the IEEE international conference on computer vision*, pages 5542–5550, 2017. [5](#), [6](#)
- [22] Pan Li, Da Li, Wei Li, Shaogang Gong, Yanwei Fu, and Timothy M Hospedales. A simple feature augmentation for domain generalization. In *Proceedings of the IEEE/CVF International Conference on Computer Vision*, pages 8886–8895, 2021. [6](#), [7](#)
- [23] Yunsheng Li, Lu Yuan, Yinpeng Chen, Pei Wang, and Nuno Vasconcelos. Dynamic transfer for multi-source domain adaptation. In *Proceedings of the IEEE/CVF Conference on Computer Vision and Pattern Recognition*, pages 10998–11007, 2021. [1](#)
- [24] Divyat Mahajan, Shruti Tople, and Amit Sharma. Domain generalization using causal matching. In *International Conference on Machine Learning*, pages 7313–7324. PMLR, 2021. [6](#)
- [25] Toshihiko Matsuura and Tatsuya Harada. Domain generalization using a mixture of multiple latent domains. In *Proceedings of the AAAI Conference on Artificial Intelligence*, volume 34, pages 11749–11756, 2020. [6](#)
- [26] Shruti Nagpal, Maneet Singh, Richa Singh, and Mayank Vatsa. Attribute aware filter-drop for bias invariant classification. In *Proceedings of the IEEE/CVF Conference on Computer Vision and Pattern Recognition Workshops*, pages 32–33, 2020. [3](#)

[27] Hyeonseob Nam, HyunJae Lee, Jongchan Park, Wonjun Yoon, and Donggeun Yoo. Reducing domain gap by reducing style bias. In *Proceedings of the IEEE/CVF Conference on Computer Vision and Pattern Recognition*, pages 8690–8699, 2021. 1, 2, 6, 12

[28] Sinno Jialin Pan and Qiang Yang. A survey on transfer learning. *IEEE Transactions on knowledge and data engineering*, 22(10):1345–1359, 2009. 1

[29] Vihari Piratla, Praneeth Netrapalli, and Sunita Sarawagi. Efficient domain generalization via common-specific low-rank decomposition. In *International Conference on Machine Learning*, pages 7728–7738. PMLR, 2020. 1, 2

[30] Mohsen Saffari, Mahdi Khodayar, Mohammad Saeed Ebrahimi Saadabadi, Ana F Sequeira, and Jaime S Cardoso. Maximum relevance minimum redundancy dropout with informative kernel determinantal point process. *Sensors*, 21(5):1846, 2021. 3

[31] Christian Schreckenberger, Christian Bartelt, and Heiner Stuckenschmidt. idropout: Leveraging deep taylor decomposition for the robustness of deep neural networks. In *OTM Confederated International Conferences “On the Move to Meaningful Internet Systems”*, pages 113–126. Springer, 2019. 3

[32] Ramprasaath R Selvaraju, Michael Cogswell, Abhishek Das, Ramakrishna Vedantam, Devi Parikh, and Dhruv Batra. Grad-cam: Visual explanations from deep networks via gradient-based localization. In *Proceedings of the IEEE international conference on computer vision*, pages 618–626, 2017. 1, 12

[33] Seonguk Seo, Yumin Suh, Dongwan Kim, Geoho Kim, Jongwoo Han, and Bohyung Han. Learning to optimize domain specific normalization for domain generalization. In *Computer Vision–ECCV 2020: 16th European Conference, Glasgow, UK, August 23–28, 2020, Proceedings, Part XXII 16*, pages 68–83. Springer, 2020. 6

[34] Shiv Shankar, Vihari Piratla, Soumen Chakrabarti, Siddhartha Chaudhuri, Preethi Jyothi, and Sunita Sarawagi. Generalizing across domains via cross-gradient training. In *International Conference on Learning Representations*, 2018. 1, 2

[35] Yang Shu, Zhangjie Cao, Chenyu Wang, Jianmin Wang, and Mingsheng Long. Open domain generalization with domain-augmented meta-learning. In *Proceedings of the IEEE/CVF Conference on Computer Vision and Pattern Recognition*, pages 9624–9633, 2021. 2, 6

[36] Nitish Srivastava, Geoffrey Hinton, Alex Krizhevsky, Ilya Sutskever, and Ruslan Salakhutdinov. Dropout: a simple way to prevent neural networks from overfitting. *The journal of machine learning research*, 15(1):1929–1958, 2014. 2

[37] Jonathan Tompson, Ross Goroshin, Arjun Jain, Yann LeCun, and Christoph Bregler. Efficient object localization using convolutional networks. In *Proceedings of the IEEE conference on computer vision and pattern recognition*, pages 648–656, 2015. 2, 3

[38] Antonio Torralba and Alexei A Efros. Unbiased look at dataset bias. In *CVPR 2011*, pages 1521–1528. IEEE, 2011. 5, 6

[39] Dmitry Ulyanov, Andrea Vedaldi, and Victor Lempitsky. Instance normalization: The missing ingredient for fast stylization. *arXiv preprint arXiv:1607.08022*, 2016. 4

[40] Dmitry Ulyanov, Andrea Vedaldi, and Victor Lempitsky. Improved texture networks: Maximizing quality and diversity in feed-forward stylization and texture synthesis. In *Proceedings of the IEEE Conference on Computer Vision and Pattern Recognition*, pages 6924–6932, 2017. 4

[41] Hemanth Venkateswara, Jose Eusebio, Shayok Chakraborty, and Sethuraman Panchanathan. Deep hashing network for unsupervised domain adaptation. In *Proceedings of the IEEE conference on computer vision and pattern recognition*, pages 5018–5027, 2017. 5, 6

[42] Riccardo Volpi, Hongseok Namkoong, Ozan Sener, John Duchi, Vittorio Murino, and Silvio Savarese. Generalizing to unseen domains via adversarial data augmentation. In *Proceedings of the 32nd International Conference on Neural Information Processing Systems*, pages 5339–5349, 2018. 1, 2

[43] Shujun Wang, Lequan Yu, Caizi Li, Chi-Wing Fu, and Pheng-Ann Heng. Learning from extrinsic and intrinsic supervisions for domain generalization. In *European Conference on Computer Vision*, pages 159–176. Springer, 2020. 1, 2, 6

[44] Zijian Wang, Yadan Luo, Ruihong Qiu, Zi Huang, and Mahsa Baktashmotagh. Learning to diversify for single domain generalization. In *Proceedings of the IEEE/CVF International Conference on Computer Vision*, pages 834–843, 2021. 2, 6

[45] Guoqiang Wei, Cuiling Lan, Wenjun Zeng, and Zhibo Chen. Metaalign: Coordinating domain alignment and classification for unsupervised domain adaptation. In *Proceedings of the IEEE/CVF Conference on Computer Vision and Pattern Recognition*, pages 16643–16653, 2021. 1, 2, 5

[46] Guile Wu and Shaogang Gong. Collaborative optimization and aggregation for decentralized domain generalization and adaptation. In *Proceedings of the IEEE/CVF International Conference on Computer Vision*, pages 6484–6493, 2021. 6

[47] Qinwei Xu, Ruipeng Zhang, Ya Zhang, Yanfeng Wang, and Qi Tian. A fourier-based framework for domain generalization. In *Proceedings of the IEEE/CVF Conference on Computer Vision and Pattern Recognition*, pages 14383–14392, 2021. 5, 6

[48] Yuyuan Zeng, Tao Dai, Bin Chen, Shu-Tao Xia, and Jian Lu. Correlation-based structural dropout for convolutional neural networks. *Pattern Recognition*, page 108117, 2021. 3

[49] Xingxuan Zhang, Peng Cui, Renzhe Xu, Linjun Zhou, Yue He, and Zheyuan Shen. Deep stable learning for out-of-distribution generalization. In *Proceedings of the IEEE/CVF Conference on Computer Vision and Pattern Recognition*, pages 5372–5382, 2021. 5, 6, 11

[50] Kaiyang Zhou, Yongxin Yang, Timothy Hospedales, and Tao Xiang. Learning to generate novel domains for domain generalization. In *European Conference on Computer Vision*, pages 561–578. Springer, 2020. 6

[51] Kaiyang Zhou, Yongxin Yang, Yu Qiao, and Tao Xiang. Domain generalization with mixstyle. In *International Conference on Learning Representations*, 2020. 5, 6, 8

A. Implementation Details

Network details. Overall, for the network implementation, we closely follow the implementations provided in [4, 12, 49]. For all the ResNet networks, we utilize the ImageNet pre-trained models as the backbones. We employ the same hyper-parameters as [4] on PACS, [49] on VLCS, and [12] on Office-Home, respectively. For all datasets, we train our network using the Nesterov-momentum SGD with a momentum of 0.9 and weight decay of 5×10^{-4} for a total of 60 epochs. In both stages, the number of epochs is set as 30 and the initial learning rate is 10^{-3} . The learning rate is decayed by 0.1 at 80% of the epochs for each stage.

Data augmentation. In this paper, we utilize two data augmentation techniques for all datasets. The first is the standard augmentation protocol as that in [4], which consists of cropping the images to retain between 80% to 100% of the original area, horizontal flipping with probability of 50%, color jittering with magnitude of 0.4, and gray scaling with probability of 10%. The second is the random augmentation as that in [7], *i.e.*, randomly selecting 8 transformations from 14 available transformations with the magnitude of each augmentation distortion as 4. Moreover, given 64 samples for each iteration, we perform the standard augmentation and the random augmentation to generate the augmented images, respectively and then combine them to form a batch with 128 samples to train the model. The input image size is 224×224 in all experiments.

B. The Choice of Hyperparameter

Sensitivity to maximum dropping proportion. P_{\max} is a hyper-parameter indicating the maximum proportion of dropping channels. We conduct the experiment with our strong baseline model, *i.e.*, DeepAll with SwapStyle and RandAugment (DeepAll⁺⁺), on VLCS and OfficeHome. The results are represented in Fig. 1. On VLCS dataset, the model achieves the best performance when P_{\max} is 0.33. Due to the small domain discrepancy on OfficeHome, P_{\max} on OfficeHome should be smaller than that on PACS and VLCS, and thus it is set as 0.25. For all datasets, setting P_{\max} as too large or too small value might lead to performance degeneration. A too large P_{\max} may cause losing too much information during training and preventing the model from learning discriminative representation from source domains, while a too small P_{\max} may lead the model to fail to adequately alleviate the overfitting issue in source domains.

C. Additional Results

Complete results of two-stages training scheme. We present the complete comparative results of the one-stage scheme and two-stages scheme in Tab. 1. Our method can obtain a larger improvement by 1.41% (86.33% vs. 84.92%) in two-stages training than the improvement of

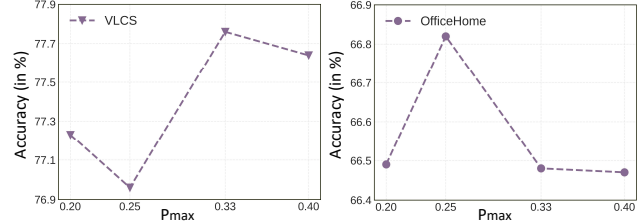


Figure 1. Performance (%) of different P_{\max} in PLACE dropout on the VLCS and OfficeHome datasets.

Table 1. Performance (%) of two-stages training scheme on the PACS dataset with ResNet-18.

Method	Art	Cartoon	Sketch	Photo	Avg.
DeepAll ⁺⁺	83.64	78.28	81.41	96.34	84.92
One-stage	84.98	79.78	82.38	96.29	85.86 ($\uparrow 0.94$)
Two-stages	84.83	80.12	83.68	96.69	86.33 ($\uparrow 1.41$)

Table 2. The distribution discrepancy ($\times 10^2$) of inter-domain (across all source domains) and intra-class (for all classes in source domains) on PACS. Note that the lower the value indicates the better performance.

Datasets	VLCS		OfficeHome	
	Inter-domain	Intra-class	Inter-domain	Intra-class
DeepAll	15.81	24.09	7.64	14.86
+ PLACE	15.44	23.50	7.12	14.39
DeepAll ⁺⁺	14.71	23.40	6.89	14.02
+ PLACE	13.80	22.71	6.27	13.62

0.94% (85.86% vs. 84.92%) in one-stage training. The experimental results demonstrate that warming up the model can obtain good initialization parameters before we train the model using our PLACE dropout, thereby it can help the model generalize better on arbitrary unseen target domain.

Feature distribution discrepancy on other datasets.

We also examine the inter-domain (across all source domains) and intra-class (inter-domain distance for the same-class samples) discrepancy on VLCS and OfficeHome datasets as reported in Tab. 2. The experimental results are consistent with the results on the PACS dataset. Compared with the original DeepAll, our strong baseline DeepAll⁺⁺ can reduce the distribution discrepancy among source domains. Moreover, our PLACE dropout can further decrease the domain discrepancy on different baselines, including the original DeepAll and our strong baseline DeepAll⁺⁺. The results prove the effectiveness of our methods to alleviate the overfitting problem in source domains, which is beneficial to reduce the intra-class and inter-domain distances among source domains.

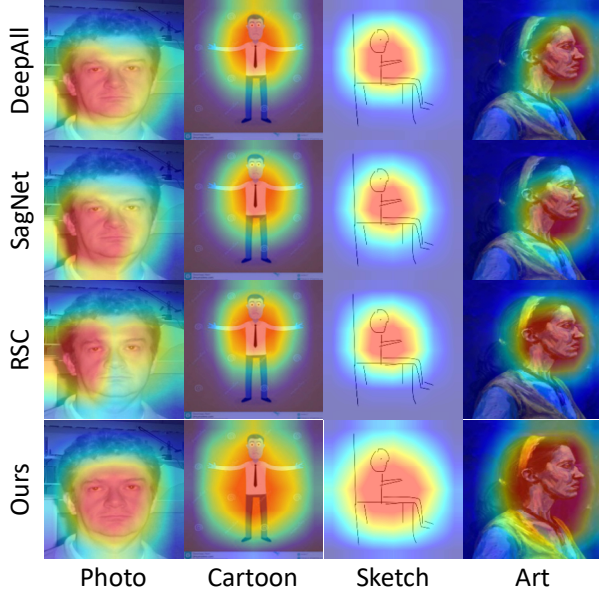


Figure 2. The Gradient-weighted Class Activation Map [32] on the PACS. Note that the redder the area indicates the higher attention. The top row is the baseline method (*i.e.*, DeepAll), the second row is the SagNet [27], the third row is the RSC [18] and the bottom row is our method PLACE. The last column is from the target domain while the first three columns are from the source domains.

D. More Visualization Results

As proved by the experiments in the paper, it is observed that PLACE dropout can significantly mitigate the overfitting problem in the source domains and promote the generalization capability of the trained model. Beyond the visualization results in the paper, we here represent several extra visualization results via Grad-CAM [32] and further explore the explanations for the effectiveness of our method. Here we utilize the ResNet-18 trained on the PACS dataset as an example, where the network is firstly trained on Photo, Cartoon, Sketch, and then evaluated on Art domain. We visualize the class activation map of the same images on DeepAll, SagNet [27], RSC [18], and our PLACE dropout, separately. The visualization results are represented in Fig. 2.

For DeepAll, we notice that the model tends to focus on the local region in source domains, *e.g.*, ‘half-face’ of person for the photo as shown in the top row of Fig. 2. This may cause the model to overfit the sample-specific or domain-specific characteristics, *i.e.*, the model is more likely to focus on the incorrect local region on the target samples and fail to correctly predict the category. The overfitting problem still exists in SagNet—one of the state-of-the-art DG methods, as shown in the second row of Fig. 2. On the contrary, our PLACE method forces the model to classify based on larger regions, *e.g.*, ‘the whole body’ of person for cartoon, which is more conducive to alle-

viate the overfitting problem. Besides, compared with the RSC method—a state-of-the-art regularization method in DG studies, we observe that the active maps of our PLACE method cover a larger area on the object than that of RSC, demonstrating that the model with PLACE dropout is capable of capturing more discriminative features.

The above experimental results demonstrate that our PLACE dropout can help the model focus on larger regions, thereby effectively alleviating the overfitting problem and improving the generalization capability of the model on arbitrary unseen domains.